MRS Advances © 2018 Materials Research Society
DOI: 10.1557/adv.2018.151

Deposition routes of $Cs_2AgBiBr_6$ double perovskites for photovoltaic applications

Martina Pantaler, Christian Fettkenhauer, Hoang L. Nguyen, Irina Anusca, and Doru C. Lupascu

Institute for Materials Science and Center of Nanointegration Duisburg-Essen (CENIDE), University of Duisburg-Essen, Universitätsstraße 15, 45141 Essen, Germany

ABSTRACT

The lead free double perovskite $Cs_2AgBiBr_6$ is an upcoming alternative to lead based perovskites as absorber material in perovskite solar cells. So far, the majority of investigations on this interesting material have focused on polycrystalline powders and single crystals. We present vapor and solution based approaches for the preparation of $Cs_2AgBiBr_6$ thin films. Sequential vapor deposition processes starting from different precursors are shown and their weaknesses are discussed. Single source evaporation of $Cs_2AgBiBr_6$ and sequential deposition of $Cs_3Bi_2Br_9$ and AgBr result in the formation of the double perovskite phase. Additionally, we show the possibility of the preparation of planar $Cs_2AgBiBr_6$ thin films by spin coating.

INTRODUCTION

Perovskite solar cells have experienced a tremendous development with an increase of power conversion efficiencies from 3.8% in 2009 [1] to 22.7% nowadays. [2] The prototype material of this low-cost alternative to silicon is methylammonium lead iodide ($CH_3NH_3PbI_3$). It possesses various beneficial properties, e.g. a direct (1.6 eV) and tunable band gap [3], a high absorption coefficient [4], long carrier diffusion lengths and lifetimes [5], high defect tolerance [6,7], high charge carrier mobility [8]. Nevertheless, there are two major disadvantages: its instability under ambient atmosphere, and the presence of toxic lead [9,10]. The first issue can be solved simply by encapsulation. Many attempts have been made to replace Pb^{2+} by isoelectronic Sn^{2+} and Ge^{2+}, or Sb^{3+} and Bi^{3+}. The latter ions usually yield low dimensional hybrid materials ($A_3^+B_2^{3+}X^-_9$) showing efficiencies ≤1.6 %. [11] Recently, bismuth based halide double perovskites have been suggested for solar cell application. Slavney et al. [12] synthesized the double perovskite $Cs_2AgBiBr_6$. Although its band gap is 1.95 eV, it possesses advantageous properties like long room temperature photoluminescence lifetime (660 ns), high defect tolerance, low hole effective masses [13,14] and higher heat and moisture stability than $MAPbBr_3$ (up to 430 °C and 55% relative humidity). [12] It crystallizes in the cubic space group Fm-3m with a lattice constant of 11.25Å. It is characterized by a 3-dimensional, alternating arrangement of corner sharing Ag^+ and Bi^{3+} centered bromide octahedra. Up to now, all reports on $Cs_2AgBiBr_6$ have been based on investigations of polycrystalline powders, single crystals, or calculations. Just recently a group succeeded to build a solar cell using mesoporous titania infiltrated with $Cs_2AgBiBr_6$. [15] We will

https://doi.org/10.1557/adv.2018.151 Published online by Cambridge University Press

discuss the preparation of planar $Cs_2AgBiBr_6$ thin films using vapor deposition and the solution based spin coating process.

EXPERIMENTAL DETAILS

Using CsBr (99.9 %), $BiBr_3$ (99.0 %), AgBr (99.5 %), and HBr (Alfa Aesar), $Cs_2AgBiBr_6$ was synthesized like reported elsewhere [14]. Metal bromides were dissolved in hydrobromic acid at 150°C for 2h, and cooled down to room temperature. The orange powder was washed with ethanol and dried overnight. $Cs_3Bi_2Br_9$ was synthesized accordingly without the addition of AgBr. The thermal vapor deposition was performed at a chamber pressure of 10^{-7} mbar (Spectros 150 system, Kurt J. Lesker). The films were annealed at 220°C for 24h in air to facilitate crystallization. Glass substrates were covered with PEDOT:PSS (Heraeus Clevios polymer dispersion) via spin coating and subsequent annealing. Spin-coating of titanium diisopropoxide bis(acetylacetonate) (0.15 M in 1-butanol; 20 s at 2800 rpm; annealing at 125°C for 5 min) was followed by spin-coating of TiO_2 paste (anatase 20 nm, Sigma Aldrich, 0.12 g/mL in 1-butanol; 20s at 2000 rpm; annealing at 125°C for 5 min). Final calcination at 550°C for 1 h leads to titania covered substrates. X-ray diffraction patterns were measured on a Siemens D5000 diffractometer (Cu Kα, 2θ 5° to 70°). Optical spectra were measured using a Shimadzu UV-VIS 2600 spectrophotometer operating from 300 to 900 nm with a step size of 1 nm. SEM/EDX measurements were carried out on the microscope Jeol JSM 7500F.

RESULTS AND DISCUSSION

The successful synthesis of $Cs_2AgBiBr_6$ was confirmed by powder X-Ray diffraction measurements (XRD) representing the cubic structure (Fm-3m) with a lattice constant of a=11.25 Å [12].

The first way to prepare the thin films was vapor deposition under high vacuum offering good thickness control and the possibility of large area surface deposition. We followed three approaches to vapor deposit $Cs_2AgBiBr_6$, which were the evaporation and deposition of $Cs_2AgBiBr_6$ itself (Fig. 1a), the sequential deposition of CsBr, AgBr, and BiBr3 (Fig. 1b), and the sequential deposition of $Cs_3Bi_2Br_9$ and AgBr (Fig. 1c). In the first case we ran the deposition at 2.5 Å/s on glass substrates at room temperature. The film is bright yellow in colour. The main reflection at 31.8° 2θ is attributed to the (400) reflection of $Cs_2AgBiBr_6$. The small XRD reflection at 15.8° 2θ can be assigned to the (200) peak of the double perovskite. One thus might assume an oriented crystal growth. The minor reflections can be attributed to BiOBr (ICPDS-ICDD no. 9-393) and AgBr (ICDD no. 00-006-0438). Apparently $Cs_2AgBiBr_6$ is not completely stable under the conditions which were present in the evaporator. This lead to partial decomposition into its binary metal bromides. During annealing, $BiBr_3$ hydrolised resulting in the BiOBr side phase.

The sequential deposition of the three binary metal bromides in 2:1:1 stoichiometry was conducted for CsBr, $BiBr_3$ and AgBr, respectively. We wanted to achieve a triple layer system which was supposed to react in the subsequent annealing step. The films are bright yellow, but do not represent $Cs_2AgBiBr_6$. Six different deposition sequences of starting materials has been conducted. Even a change in the order of the deposited layers did not lead to a successful formation of the double perovskite which we observed on the XRD diffractogram (Fig. 1b). The last attempt was to use sequential deposition of the ternary metal bromide, $Cs_3Bi_2Br_9$, which is supposed to be thermodynamically more stable than $Cs_2AgBiBr_6$,[16] followed by the deposition

https://doi.org/10.1557/adv.2018.151 Published online by Cambridge University Press

of AgBr layer and annealing to facilitate interdiffusion and reaction of the two layers. The first deposited layer was AgBr with deposition rate of 0.8 Å/s followed by $Cs_3Bi_2Br_9$ with deposition rate of 3 Å/s.The films appear darker already (Fig. 1c). Presence of main reflections (111, 200, 220, 311, 222, 400, 422, and 444), prove the successful formation of double perovskite phase. Nevertheless, impurities of AgBr and BiOBr still remain.

In summary preliminary attempts on vapor deposition for the preparation of $Cs_2AgBiBr_6$ thin films can be promising. To improve formation of pure $Cs_2AgBiBr_6$ double perovskite phase, co-evaporation of starting materials, substrate heating during vapor deposition, and post-annealing will be investigated. The lower thermodynamic stability of the double perovskite compared to some of the side phases (e.g. AgBr, $Cs_3Bi_2Br_9$) make a proper control of deposition parameters (deposition rate, pressure) necessary.

An alternative approach for the deposition of $Cs_2AgBiBr_6$ thin films is a solution based spin coating process. We conducted solubility tests of $Cs_2AgBiBr_6$ in different organic solvents. The concentration must be as high as possible in order to achieve reasonable film thicknesses. The highest solubility (0.52 mol/L) was achieved in dimethylsulfoxide (DMSO) at 70°C, which is slightly lower than the reported solubility of 0.6 M.[15] Unlike reference [15] the pre-synthesized double perovskite, $Cs_2AgBiBr_6$ solution has been used as precursor solution for spin coating. The superior solvent properties of DMSO can be understood considering its high relative permittivity ($\varepsilon_r = 46.6$ [17]) and strong Lewis acidity. Furthermore, we could observe a sequential dissolution process which resulted in a colour change from orange to yellow to white prior to complete dissolution of the powder resulting in a yellow solution. Accordingly, we assume first the dissolution of $BiBr_3$ followed by AgBr and CsBr.

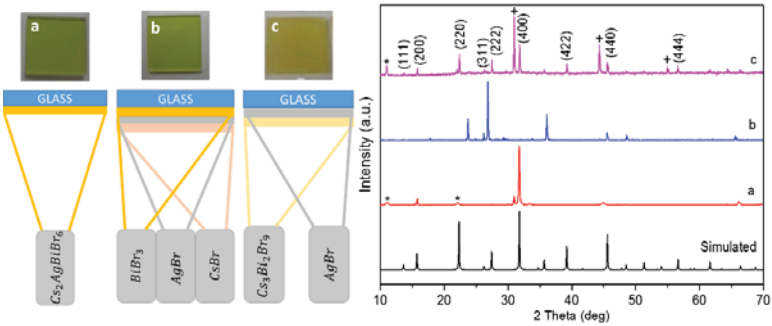

Figure 1. Schematic representation of the investigated sequential vapor deposition processes, images, and XRD pattern of the resulting films; a) deposition of $Cs_2AgBiBr_6$, b) $BiBr_3$ – AgBr – CsBr, and c) $Cs_3Bi_2Br_9$ – AgBr. *BiOBr; +AgBr

In order to optimize the thin film morphology with respect to its homogeneity, smoothness, and thickness, we investigated the influence of rotational speed (2500 rpm - 5000 rpm), atmosphere (dry N_2 and ambient atmosphere), and heat treatment during spin coating. We found that processing under ambient atmosphere leads to thin films appearing turbid and light scattering whereas processing in dry nitrogen resulted in translucent films. Additionally, the spin coating process at 4000 rpm for 30 seconds was found to be the best as estimated from macro- and microscopic investigations. We performed a subsequent annealing step under nitrogen in order to induce crystal growth in the films. Annealing at 120°C after deposition hardly shows any regular particles of

https://doi.org/10.1557/adv.2018.151 Published online by Cambridge University Press

around 50 nm in size (Figure 2a). Annealing at 220°C after spin coating causes the formation of larger grains with broader size distribution due to rapid evaporation of the solvent.(Figure 2b) The optimal treatment is to gradually increase the annealing temperature from 120°C to 220°C (3 °C min^{-1}) which results in spherical particles with narrow size distribution (100 nm). The thickness of the films is about 200 nm.(Figure 2c)

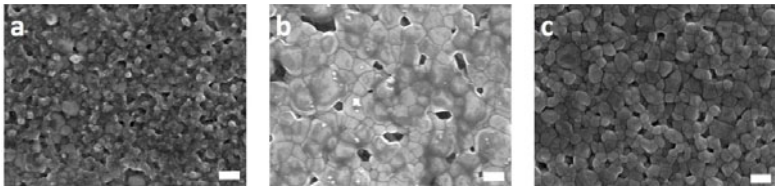

Figure 2. SEM images of $Cs_2AgBiBr_6$ thin film surfaces after annealing at a) 120°C, b) 220°C, and c) 120 °C to 220°C (scale bars: 200nm).

The thin films were prepared both on PEDOT:PSS and on mesoporous titania, because these are the commonly used hole and electron transporting layers in solid state perovskite solar cells. XRD and EDX analysis prove successful formation of the double perovskite phase with stoichiometry $Cs_{2.07}Ag_{1.18}Bi_{0.93}Br_6$ in both cases (Fig. 3a). Comparing the Tauc-Plot of both the thin film and the double perovskite powder we see a blue-shift of the absorption edge with band gap of 2.42 eV (Fig. 3b). This is probably caused by the low film thickness and particle size and/or remaining amorphous parts in the thin film. The difference to the reported value of 2.21 eV for a thin film [15] can be explained by higher film thickens due to higher precursor concentration and lower spin coating speed (2000 rpm at 30 s).

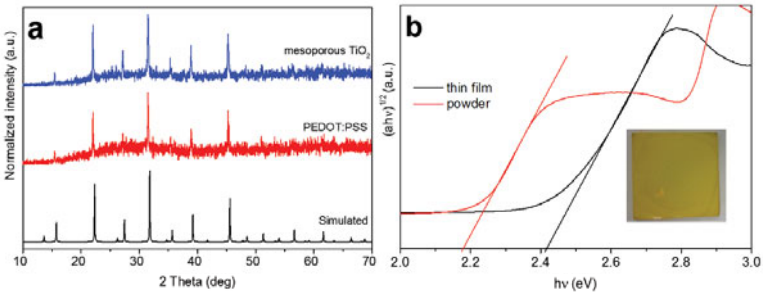

Figure 3. a) XRD $Cs_2AgBiBr_6$ deposited on different sublayers, and b) Tauc-plots of $Cs_2AgBiBr_6$ thin film (right curve) and powder (left curve).

https://doi.org/10.1557/adv.2018.151 Published online by Cambridge University Press

CONCLUSION

In summary, we showed the application of physical vapor deposition to obtain $Cs_2AgBiBr_6$ thin films. It turned out that, so far, the vapor deposition of $Cs_2AgBiBr_6$ itself and a two-step sequential deposition process of $Cs_3Bi_2Br_9$ and AgBr can be promising approaches. Alternatively, solution processing of $Cs_2AgBiBr_6$ dissolved in DMSO is possible under inert atmosphere and allows for the preparation of smooth and homogenous planar thin films. Therefore ongoing work is focussing on the construction of a working planar perovskite solar cell which will be published in an upcoming paper.

ACKNOWLEDGMENTS

C.F., M.P., and D.C.L. acknowledge financial support through the European Union via the Leitmarktwettbewerb NRW: Neue Werkstoffe, project EFRE-0800120; NW-1-1-040h; I.A. through BMBF project 03SF0517A. Svetlana Sirotinskaya is kindly acknowledged for the SEM measurements and the PeroBOOST teams for discussions.

REFERENCES

1. A. Kojima, K. Teshima, Y. Shirai, and T. Miyasaka, *J. Am. Chem. Soc.* **131** 6050–6051 (2009).
2. National Renewable Energy Laboratory (NREL) Efficiency Chart**.** Available at: https://www.nrel.gov/pv/assets/images/efficiency-chart.png (accessed 30 October 2017)**.**
3. T.M. Brenner, D.A. Egger, L. Kronik, G. Hodes, and D. Cahen, *Nat. Rev. Mater.* 1 15007 (2016).
4. J.H. Noh, S.H. Im, J.H. Heo, T.N. Mandal, and S.I. Seok, *Nano. Lett.* 13, 1764 (2013).
5. S.D. Stranks, G.E. Eperon, G. Grancini, C. Menelaou, M.J.P. Alcocer, T. Leijtens, L.M. Herz, A. Petrozza, H.J. Snaith, *Science* 342, 341-344 (2013).
6. R.E. Brandt, V. Stevanovic, D.S. Ginley, and T. Buonassisi, *MRS Commun.* 5, 265−275 (2015).
7. I. Anusca, S. Balciunas, P. Gemeiner, S. Svirskas, M. Sanlialp, G. Lackner, C. Fettkenhauer, J. Belovickis, V. Samulionis, M. Ivanov, B. Dkhil, J. Banys, V.V. Shvartsman, and D.C. Lupascu, *Adv. Energy Mater*. 7, 1700600 (2017).
8. C. Wehrenfennig, G.E. Eperon, M.B. Johnston, H.J. Snaith, and L.M. Herz, *Adv. Mater.* 26, 1584−1589 (2014).
9. N. Aristidou, I. Sanchez-Molina, T. Chotchuangchutchaval, M. Brown, L. Martinez, T. Rath, and S.A. Haque, *Angew. Chem., Int. Ed.* 54, 8208−8212 (2015).
10. A. Babayigit, A. Ethirajan, M. Muller, and B. Conings, *Nat. Mater.* 15, 247− 251 (2016).
11. Zheng Zhang, Xiaowei Li, Xiaohong Xia, Zhuo Wang, Zhongbing Huang, Binglong Lei, and Yun Gao, *J. Phys. Chem. Lett*. 8 (17), 4300–4307 (2017).
12. A.H. Slavney, Te Hu, A.M. Lindenberg, and H.I. Karunadasa, *J. Am. Chem. Soc*. 138 (7), 2138–2141 (2016).
13. E.T. Mcclure, M.R. Ball, W. Windl, and P.M. Woodward, *Chem. Mater*. 28, 1348−1354 (2016).
14. G. Volonakis, M.R. Filip, A.A. Haghighirad, N. Sakai, B. Wenger, H. J. Snaith, and F. Giustino, *J. Phys. Chem. Lett*. 7, 1254-1259 (2016).
15. E. Greul, M.L. Petrus, A. Binek, P. Docampo, and T. Bein, *J. Mater. Chem. A*. 5, 19972 (2017).
16. Z. Xiao, W. Meng, J. Wang, Y. Yan, *ChemSusChem* 9, 2628-2633 (2016)
17. I.M. Smallwood, *Handbook of organic solvent properties* (Arnold, London, 1996) p. 253.

https://doi.org/10.1557/adv.2018.151 Published online by Cambridge University Press